energies

MDPI

Article

A Compact and High-Power Rectenna Array for Wireless Power Transmission Applications

Dajiu Huang [1], Jincheng Li [2], Ziqiang Du [1], Changjun Liu [2], Zhongqi He [2] and Ji Zhang [1,*]

[1] China Telecom Group Co., Ltd. Sichuan Branch, Chengdu 610015, China
[2] College of Electronics and Information Engineering, Sichuan University, Chengdu 610064, China
* Correspondence: zhangji@sctel.com.cn

Abstract: Microwave wireless power transmission (MWPT) applications have attracted worldwide interest and attention in recent years. Rectennas are a crucial component of a MWPT system. The rectenna's power capacity and output DC power have great significance with regard to the MWPT system's performance. In this article, a compact 4 × 4 S-band rectangular patch rectenna array for MWPT is proposed and experimentally verified. Firstly, an S-band rectifier with better consistency and lower cost than a traditional output design using parallel capacitors as a filter is achieved. Then, a rectenna array based on the proposed rectifier and a novel design idea is proposed. The rectenna can achieve an output DC power of 117.6 mW/cm^3 and an efficiency of 47.6%. Finally, a MWPT verification experiment is conducted. A 12-inch LCD screen powered by the rectenna with a rated power of 12 W successfully works without any other power supply. This article provides a new design of a rectenna for MWPT, and the proposed rectenna array demonstrates its good engineering significance and application prospects.

Keywords: antenna array; compact; high-power; rectifier; rectenna; S-band; wireless power transmission

Citation: Huang, D.; Li, J.; Du, Z.; Liu, C.; He, Z.; Zhang, J. A Compact and High-Power Rectenna Array for Wireless Power Transmission Applications. *Energies* **2024**, *17*, 6008. https://doi.org/10.3390/en17236008

Received: 16 October 2024
Revised: 5 November 2024
Accepted: 11 November 2024
Published: 29 November 2024

1. Introduction

Since Nikola Tesla introduced the concept of electromagnetic wireless power transmission in the late 19th century with his attempt to construct the Wardenclyffe Tower [1], wireless power transmission (WPT) technology has undergone over a century of advancement. Numerous scientists, engineers, and researchers have continually explored methods to enable device power delivery without the need for physical cables. Reliable WPT technology offers effective solutions to the limitations of wired connections in complex or harsh environments. Notable applications include the transmission of power from space-based solar power stations to Earth [2–4], the wireless powering of drones and pipeline robots [5,6], and providing power to remote or island-based unmanned radar stations [7]. Microwave wireless power transmission (MWPT) technology, with its resilience to environmental factors, extended transmission distances, and support for higher power levels, represents a crucial direction for the future evolution of WPT technology.

As the primary receiving and converting device in MWPT systems, the rectenna significantly impacts the system's overall performance. To ensure effective wireless power transmission, the rectenna must meet specific size, efficiency, and power capacity requirements. Common rectenna systems typically consist of an antenna and a rectifier, where the efficiency of the rectifier directly affects the rectification efficiency of the rectenna. Consequently, researchers are dedicated to creating better-performing rectifiers. A single diode rectifier circuit with a series band-stop structure has been proposed [8], which utilizes a segment of microstrip line to simultaneously achieve impedance matching and harmonic suppression, ultimately achieving 80.9% rectification efficiency at 20 dBm, while enabling the miniaturization and high efficiency of the rectifier circuit. Additionally, Roberg et al. have developed a traditional Class C rectifier operating at 2.45 GHz using a harmonic load

network method, achieving a maximum efficiency of 72.8% at an input power of 8 dBm [9]. Additionally, multi-frequency [10,11], wideband [12], and large-dynamic-range [13,14] rectifiers have attracted considerable attention.

Further advancements in compact and high-efficiency rectennas have been achieved through optimized antenna designs and impedance characteristics. Hu et al. proposed a dual-beam rectenna based on a short series-coupled traveling wave patch array to allow power to be received from a wide range of angles [15]. By directly conjugate-matching the diode with a patch antenna, Liu et al. simplify the impedance-matching network and avoid additional insertion loss to achieve high-efficiency rectennas [16]. Additionally, there are also plenty of works that focus on designing high-gain antennas [17] to enhance the antennas' ability to receive electromagnetic waves, or on achieving simple matching network [18,19], multi-frequency [20], wideband [21], and wide-input-range antennas [22] to meet the demand for power transmission. Additionally, multi-tone rectifiers [23–25] and rectennas [26] have been explored to meet the needs of different scenarios.

Improving the efficiency of microwave wireless power transmission remains an important topic. There is still significant room to increase the power capacity of microwave wireless power transmission systems. Moreover, comprehensive validation of wireless power transmission systems is still rarely reported. To address these challenges, this paper proposes a compact, high-power rectenna to improve the efficiency, compactness, and power capacity of wireless power transmission. In this design, a serpentine microstrip thin-line output filter, offering better consistency and lower manufacturing costs, is used. Microstrip lines are employed to match the rectangular microstrip patch antenna with the rectifier, resulting in a 4×4 compact rectenna array. A wireless power transmission system was built using a magnetron high-power microwave source, successfully powering a 12 W LCD screen at a distance of 2 m from the proposed rectenna array. This system validated the wireless power transmission link and demonstrated the effectiveness of the proposed rectenna array.

2. Design of Rectifier with Serpentine Microstrip-Line Filter

In a microwave wireless power transmission system, the rectenna is located at the receiving end of the system. A common rectenna mainly comprises a receiving antenna, a matching circuit, and a rectifier. When designing a rectenna, unlike in conventional antenna design, it is necessary to consider not only the antenna's performance parameters, such as radiation pattern, gain, polarization, and VSWR, but also the rectifier design. The performance of the rectifier significantly impacts the overall rectification efficiency and power capacity of the rectenna. This section will focus on the design methods for the rectifier.

2.1. Principle of Recitfiers

The equivalent circuit model of a Schottky diode is shown in Figure 1. This model involves both the parasitic and intrinsic parameters of the Schottky diode, as well as equivalent parameters introduced by the package. In this equivalent model, L_s and C_g represent the equivalent series inductance and equivalent parallel capacitance caused by the diode package, respectively. R_s is the parasitic series resistance of the Schottky diode, which is the sum of the resistances of different parts of the Schottky junction. C_j is the junction capacitance composed of the Schottky barrier junction capacitance and diffusion capacitance [27]. It can be seen that the operating characteristics of the Schottky diode are mainly determined by the diode's intrinsic parameters, R_j and C_j.

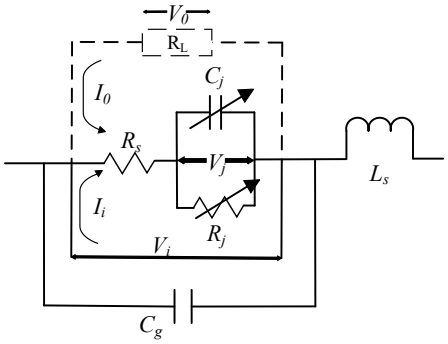

Figure 1. The equivalent circuit model of a Schottky diode.

When the input voltage V_i of the Schottky diode is

$$V_i = -V_{DC} + V_p \cos \omega t \tag{1}$$

where V_p is the voltage amplitude of the input AC signal and V_{DC} is the output DC voltage of the microwave rectifier, which is equivalent to applying a reverse bias to the Schottky diode, the junction voltage V_j can be

$$V_j = \begin{cases} -V_{j0} + V_{j1} \cos(\omega t - \varphi), & V_j < V_{bi} \\ V_{bi}, & V_j > V_{bi} \end{cases} \tag{2}$$

V_{bi} is the forward voltage drop of the diode when the diode is on. According to Equation (2), under normal operating conditions, the Schottky diode typically oscillates between conducting and non-conducting states. When the junction voltage of the diode exceeds the forward conduction voltage, the diode is in the conducting state, and the conduction angle θ_{on}, in radian, can be expressed as follows:

$$\tan \theta_{on} - \theta_{on} = \frac{\pi R_s}{R_L \left(1 + \frac{V_{bi}}{V_{DC}}\right)} \tag{3}$$

The smaller the conduction angle, the lower the power loss in the Schottky diode [28]. When a Schottky diode operates under a high-power RF signal, due to the nonlinearity of its junction capacitance C_j, the diode not only responds to the fundamental frequency but also generates higher-order harmonics. Researchers have conducted research on harmonic models in WPT applications [29]. The nonlinearity of the Schottky diode's junction capacitance can be expressed as follows:

$$C_j = C_0 + C_1 \cos(\omega t - \varphi) + C_2 \cos(2\omega t - 2\varphi) + \cdots \tag{4}$$

It can be seen that Schottky diodes often generate higher-order harmonics under high RF signal inputs. Since microwave power is primarily concentrated in the fundamental frequency, second harmonic, and third harmonic, when creating simulations and designs that incorporate Schottky diodes, it is necessary to account for the impact of at least the third harmonic on the circuit. To address the generation of higher-order harmonics, filters should be employed to eliminate these unwanted signals and recover their power for reuse. This approach helps mitigate the negative impact of harmonics and enhances the rectification efficiency of the diode.

In addition, according to Professor Kai Chang's work [30], in a microwave rectifier, microwave energy is primarily converted into DC power and losses by the rectifier. The losses of microwave energy include (1) $P_{Loss,on,Rs}$: losses caused by the series resistance R_S of the Schottky diode when it is in the forward conduction state, as current flows through the resistance. (2) $P_{Loss,junction}$: losses on the Schottky junction of the diode when it is

in the forward conduction state. (3) $P_{Loss,off,Rs}$: losses caused by the series resistance R_S of the Schottky diode when it is in the reverse cutoff state, due to leakage current. The losses and the junction capacitance C_j of the rectifying diode can be expressed by the following calculation:

$$P_{Loss} = P_{Loss,on,Rs} + P_{Loss,junction} + P_{Loss,off,Rs} \tag{5}$$

$$P_{Loss,on,R_s} = \frac{1}{2\pi}\int_{-\theta_{on}}^{\theta_{on}} \frac{(V_i - V_{bi})^2}{R_s} d\theta \tag{6}$$

$$P_{Loss,off,R_s} = \frac{1}{2\pi}\int_{\theta_{on}}^{2\pi-\theta_{on}} \frac{(V_i - V_j)^2}{R_s} d\theta \tag{7}$$

$$P_{Loss,Junction} = \frac{1}{2\pi}\int_{-\theta_{on}}^{\theta_{on}} \frac{V_i - V_{bi}}{R_s} \cdot V_{bi} d\theta \tag{8}$$

$$C_j = C_{j0}\sqrt{\frac{V_{bi}}{V_{bi} + |V_0|}} \tag{9}$$

Therefore, the rectification efficiency of the microwave rectifier can ultimately be expressed as follows:

$$\eta = \frac{P_{DC}}{P_{MW}} = \frac{P_{DC}}{P_{DC} + P_{Loss}} \tag{10}$$

In the design and simulation of microwave rectifiers, factors such as operating frequency, microwave-to-DC conversion efficiency, power capacity, and Schottky diode losses are considered. It is essential to select appropriate Schottky diodes, the corresponding number of diodes, and circuit structures to enhance the performance of the rectifier.

2.2. Design and Analysis of Desired Rectifier

Based on the previous analysis and considering the required output power, the rectifier designed in this paper adopts a voltage-doubling rectifier configuration. Figure 2 provides a schematic diagram of the rectifier based on two Schottky diodes. This circuit employs a voltage-doubling rectification method to increase the power capacity and output voltage of the circuit.

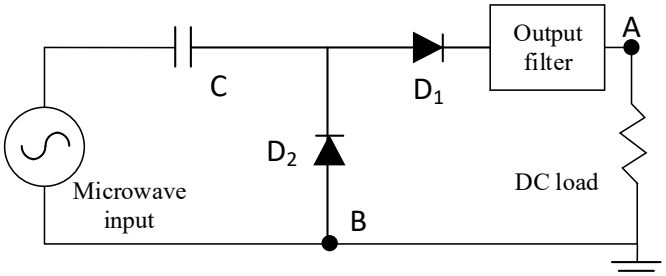

Figure 2. Schematic diagram of a common rectifier.

The main components of a voltage-doubling circuit typically consist of two Schottky diodes, D_1 and D_2, along with a series capacitor C. The DC output voltage of a microwave voltage-doubling rectifier is ultimately applied to the series loop of the two Schottky diodes (connected at points A and B). As a result, the voltage-doubling structure allows the rectifier's voltage rating and power capacity to be increased to twice that of a single-diode microwave rectifier. After careful consideration of the circuit's input power, frequency, and other parameters, the diode selected for this rectifier is the HSMS-2700 Schottky diode from Avago Technologies, San Jose, CA, USA. Its main parameters are shown in Table 1.

Table 1. Partial parameters of HSMS-2700 Schottky diode.

	Reverse Break Voltage	Junction Capacitance	Series Resistance
Symbol	V_{br}	C_{j0}	R_s
Value	25 V	6.7 pF	0.65 Ω

The input section of a microwave-voltage multiple rectifier primarily serves the functions of circuit matching, band-pass filtering, and charging/discharging. The input end typically uses a filter capacitor as the main component, and an impedance-matching network is achieved through microstrip lines to meet the requirements of the input network for the proposed rectifier. This capacitor simultaneously performs the functions of voltage multiplication and filtering.

The output network of the microwave voltage-doubling rectifier primarily consists of an output DC-pass filter and a matching circuit. The commonly used DC-pass filter at the output of a microwave rectifier is shown in Figure 3. It is mainly composed of microstrip stub lines and parallel capacitors.

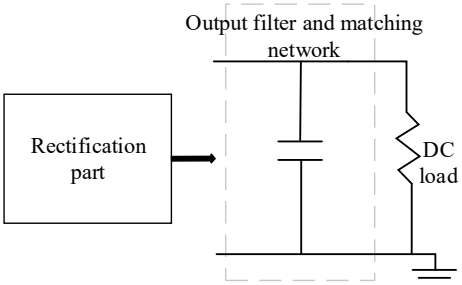

Figure 3. Schematic diagram of a commonly used output DC-pass filter structure for microwave rectifiers.

This rectifier is proposed to enable reliable wireless power transmission, which requires the integration of a high-power capacity and a larger DC-output power antenna array. The introduction of the rectenna array increases the number of rectifiers needed, thereby placing higher demands on circuit consistency. Based on experiences related to microwave rectifier design and experimental engineering, the main factors affecting rectifier consistency are as follows: (1) Soldering errors of rectifying diodes and other surface-mount components; (2) the stability of the dielectric substrate material; (3) precision in the fabrication of microstrip lines; (4) the manufacturing accuracy of diodes and other surface-mount components. Therefore, during batch design and experimentation of rectifiers, circuit consistency becomes a crucial factor to consider. Maintaining a high level of circuit consistency will minimize energy loss in the microwave rectifier.

Based on the above analysis, to improve the consistency of the rectifier, reduce the impact of surface-mount components on microwave energy loss, and minimize the size of the filter, this paper adopts a serpentine microstrip thin line as the output filter for the microwave rectifier. By adjusting the length and width of the parallel microstrip lines, an output filter with a serpentine thin line width of 0.2 mm is ultimately obtained. The rectifier structure based on this output filter is shown in Figure 4b. For comparison, Figure 4a also presents the rectifier structure with a capacitor as the filter.

After the PCB design and manufacturing process, three units of each of the two rectifier designs shown in Figure 5 were obtained. Figure 5a shows the microwave rectifier with a surface-mount capacitor as the core of the output filter. The main structure of this rectifier is as follows: (1) Part A: input filtering and matching circuit, consisting of a 0.7 pF Murata capacitor and a matching stub line. (2) Part B: the rectification section, which is composed of a matching stub line and two HSMS-2700 Schottky diodes. The two diodes form a voltage-doubling structure to increase power capacity and DC output power. (3) Part C: output DC-pass filter, consisting of a matching stub line and a 70 pF

Murata capacitor. Figure 5b shows the microwave rectifier with a serpentine microstrip line as the core of the output filter. Its main structure is as follows: (1) Part A comprises input filtering and a matching circuit, also composed of a 0.7 pF Murata capacitor and matching stub line. (2) Part B is the rectification section, with a design similar to that depicted in Figure 5a, consisting of a matching stub line and two HSMS-2700 Schottky diodes in a voltage-doubling configuration for increased power capacity and DC output power. (3) Part C is an output low-pass filter composed of a matching stub line and a high-impedance serpentine microstrip thin line.

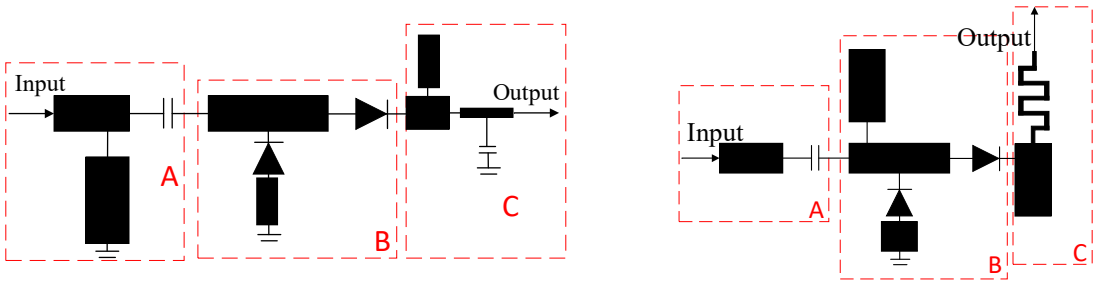

(**a**) (**b**)

Figure 4. Diagrams of (**a**) the rectifier with a parallel surface-mount capacitor as the output filter and (**b**) the rectifier with a serpentine microstrip line as the output filter.

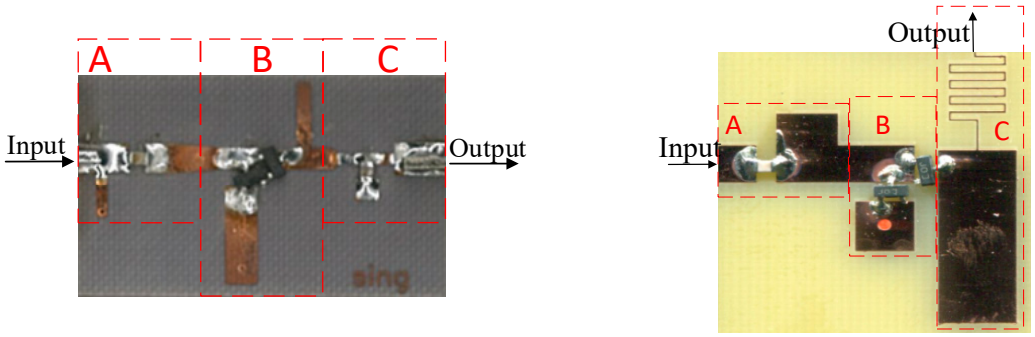

(**a**) (**b**)

Figure 5. Photographs of (**a**) the rectifier with a parallel surface-mount capacitor as the output filter and (**b**) the rectifier with a serpentine microstrip line as the output filter.

A microwave rectifier test system was set up to verify the effectiveness of the proposed circuit, as shown in Figure 6. The test system operates at a frequency of 2.45 GHz, with the signal source being an Agilent E8267C, which is capable of generating a maximum microwave power of 24 dBm. Since the tested microwave rectifier has a large power capacity, a power amplifier is used to amplify the microwave signal generated by the signal source before testing the rectifier. The DC load consists of two tunable resistor boxes. To prevent the output DC signal from exceeding the rated power of a single resistor box, the two resistor boxes are connected in series.

The results for the maximum DC output power and optimal rectification efficiency of the rectifier with a parallel surface-mount capacitor as the output filter and the serpentine microstrip line output filter rectifier at various input power levels are shown in Figure 7. The experiment results show that for the microwave rectifier with a surface-mount capacitor as the core of the output filter, the rectification efficiency exceeds 50% when the input power is between 29 dBm and 32 dBm. At an input power of 32 dBm, the rectifier achieves its highest rectification efficiency of 57.0%. Simultaneously, at this input power, the circuit delivers a maximum DC output power of 0.89 W. In addition, as shown in Figure 7b, for the microwave rectifier with a serpentine microstrip line as the core of the output filter, the

rectification efficiency exceeds 50% when the input power is between 28 dBm and 32 dBm. The highest rectification efficiency of 57.6% is achieved at an input power of 32 dBm, and the maximum DC output power of 0.93 W is obtained at an input power of 33 dBm.

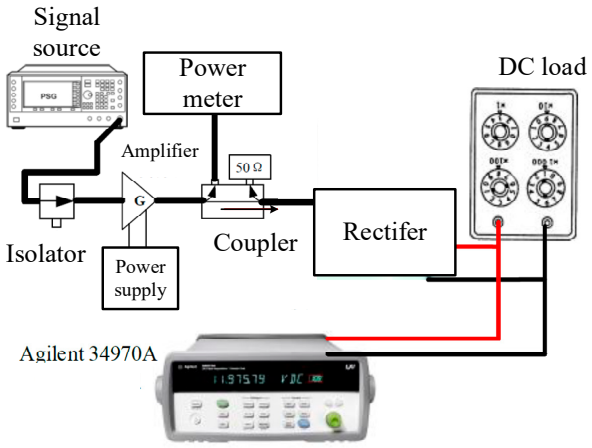

Figure 6. Diagram of rectifier measurement system.

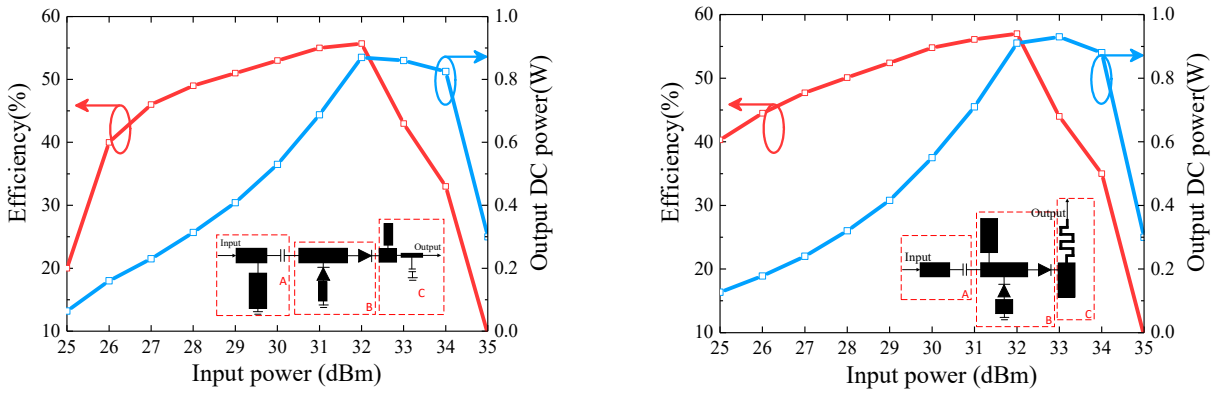

Figure 7. Measurement results of (**a**) the rectifier with a parallel surface-mount capacitor as the output filter and (**b**) the rectifier with a serpentine microstrip line as the output filter.

The final statistics of the maximum DC output power, highest rectification efficiency, circuit size, and output DC power per unit area for both microwave rectifiers are shown in Table 2. It is evident that, due to the microwave power losses associated with the surface-mount capacitor at the output, the rectifier using the capacitor as the output filter achieves a worse performance in terms of DC output power and rectification efficiency compared to the rectifier using a serpentine microstrip line as the output filter. The rectifier with a serpentine microstrip line as the filter achieves nearly 20% higher maximum DC output per unit area compared the rectifier with a capacitor as the filter.

Table 3 provides a comparison between the proposed rectifier circuit and those from other studies. It can be seen that the proposed design achieves a higher maximum DC output and can withstand greater input power, making it suitable for meeting the power demands of devices in WPT applications. The rectifier with a serpentine microstrip line as the filter, designed in this chapter, reduces the impact of surface-mount components on microwave power and offers advantages in terms of DC output power and rectification efficiency. Additionally, by incorporating the serpentine microstrip line, the manual soldering process for surface-mount capacitors is eliminated during PCB fabrication, which improves the consistency of the rectifier.

Table 2. Performance statistics of the two microwave rectifiers.

	Maximum DC Output Power	Maximum Rectification Efficiency	Size	Maximum Output DC Power per Unit Area
Rectifier with a capacitor as output filter	0.89 W	57.0%	35.4 × 25.0 mm^2	100.6 mW/cm^2
Proposed rectifier	0.93 W	57.6%	27.3 × 28.0 mm^2	121.7 mW/cm^2

Table 3. Comparison of diode-based rectifier's performance.

	Center Frequency	Maximum Rectification Efficiency	Input Power at Best Efficiency	Maximum DC Output Power	Consistency
[31]	2.45 GHz	67.7%	27.5 dBm	0.72 W	Not Considered
[32]	2.45 GHz	80.2%	25 dBm	0.5 W	Not Considered
[33]	2.45 GHz	80%	27 dBm	0.76 W	Not Considered
This work	2.45 GHz	57.6%	32 dBm	0.93 W	Considered

3. Design of Compact Rectangular Patch Rectenna Array

When designing a rectenna, similar to the procedure when designing a conventional antenna, the first consideration is the operating frequency band, which corresponds to the main operating frequency of the rectifier. The design must meet basic parameters such as radiation pattern, antenna gain, and return loss. Microstrip patch antennas offer advantages such as a simple structure, ease of fabrication and integration, and straightforward impedance matching, and as a result, they are widely used in microwave communication, wireless power transmission, and microwave measurement fields. Therefore, to ensure the reliability of the designed antenna, this design opts for a rectangular patch antenna, which has a well-established theoretical and experimental foundation for simulation and experimentation.

3.1. Antenna Design

3.1.1. Antenna Unit Design

As shown in Figure 8, the geometric parameters of a rectangular patch antenna include the width W, length L, feed width W_0, and the thickness h of the dielectric substrate, where h = 2 mm. When the rectangular microstrip patch antenna operates near its central frequency, the actual operating length L_p of the antenna is given as follows:

$$L_p = \frac{\lambda_p}{2} = \frac{c}{2f_0\sqrt{\varepsilon_e}} \tag{11}$$

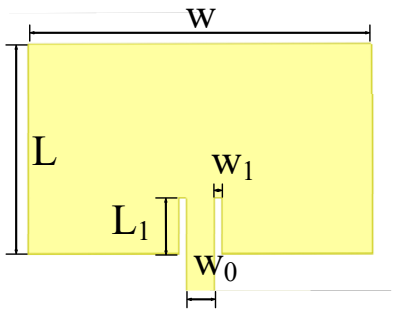

Figure 8. Structure of a patch antenna.

In the equation, λ_p is the wavelength of the microwave in the dielectric substrate, f_0 is the operating frequency of the rectangular microstrip patch antenna, and ε_e is the effective dielectric constant. The expression for the effective dielectric constant ε_e is shown below:

$$\varepsilon_e = \frac{\varepsilon_r + 1}{2} + \frac{\varepsilon_r - 1}{2}\left(1 + \frac{12h}{w}\right)^{-1/2} \tag{12}$$

When the antenna operates in a resonant state, it can be considered that each end of the antenna has a radiation slot with a length of ΔL. Therefore, the relationship between the geometric length and the actual operating length L_p of the antenna can be expressed as follows:

$$L_p = L + 2\Delta L \tag{13}$$

The length of the radiation slot ΔL is given by an empirical formula:

$$\Delta L = 0.412h\frac{\varepsilon_e + 0.3}{\varepsilon_e - 0.258}\frac{(w/h) + 0.264}{(w/h) + 0.8} \tag{14}$$

Therefore, the geometric length L of the rectangular microstrip patch antenna can be expressed as follows:

$$L = \frac{c}{2f_0\sqrt{\varepsilon_e}} - 2\Delta L \tag{15}$$

The width W of a rectangular patch antenna is generally determined by the following formula:

$$w = \frac{c}{2f_0}\left(\frac{\varepsilon_r + 1}{2}\right)^{-1/2} \tag{16}$$

After calculation, the geometric parameters of the rectangular patch antenna are determined as follows: the width W is 47.3 mm, the length L is 28.8 mm, and the feed width W_0 is 5.4 mm.

The obtained geometric parameters of the antenna are input into HFSS for preliminary modeling and simulation optimization. The final result is a rectangular microstrip patch antenna with a center frequency of 2.45 GHz. The parameters of the antenna obtained from the simulation optimization and theoretical calculations are shown in Table 4. The simulation curve of $|S_{11}|$ for the antenna is shown in Figure 9, indicating that the operating center frequency of the antenna is 2.45 GHz and the bandwidth of the antenna ranges from 2.42 GHz to 2.48 GHz.

Table 4. Parameters of the 2.45 GHz rectangular patch antennas.

	L	W	W_0	W_1	L_1
Calculated	28.8 mm	47.3 mm	5.4 mm	-	-
Simulation optimized	28 mm	46 mm	5.4 mm	1 mm	7.5 mm

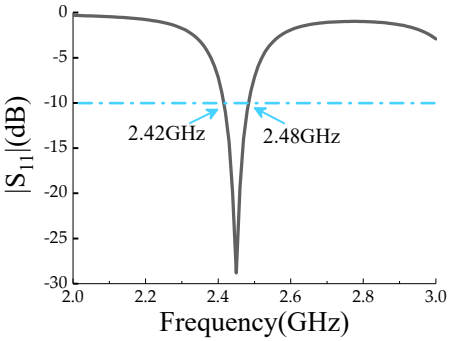

Figure 9. Simulated $|S_{11}|$ of the rectangular patch antenna.

3.1.2. Antenna Array Design

To increase the power capacity of the receiving system and enhance the DC output power at the receiving end, the antenna designed in the previous section will be arranged into an array. This will be combined with rectifiers to complete the rectenna array design. This paper intends to use the designed rectenna array to power an LCD screen. The LCD screen has a rated power of 12 W. Based on the results obtained for the designed microwave rectifiers, a total of 16 rectenna elements are needed for the array. Therefore, a 4×4 antenna array structure is proposed for this design.

Considering manufacturing costs, the area of the rectenna array should be minimized while ensuring that the coupling between antenna elements is sufficiently low to avoid mutual coupling, allowing for a more compact arrangement of the rectenna elements. The microstrip grid array antenna has the advantages of high gain, good directivity, and a simple feed structure that is conducive to integration. The radiating elements are composed of rectangular patch networks, with each rectangular patch network functioning as an individual radiating element. These rectangular patch networks are arranged in an interleaved manner, ensuring that the radiating edges of the networks do not interfere with each other while the transmission edges remain closely spaced.

To achieve a high-performance antenna array, this study proposes a microstrip patch antenna array with a unit arrangement based on the structural characteristics of the microstrip grid antenna. A typical schematic of a microstrip grid array antenna structure is shown in Figure 10a. The radiating elements of the microstrip grid array antenna are composed of rectangular patch networks, with each rectangular patch network functioning as a patch radiating element. These rectangular patch networks are arranged in a staggered configuration, ensuring that the radiating edges of adjacent networks do not interfere with each other, while the transmission edges are placed in close proximity. The structure of the proposed patch antenna array is shown in Figure 10b, where the distances between the radiating edges are denoted as w_{21} and w_{23}, and the transmission edge distance is denoted as w_{22}. Scatter parameter simulations are performed for each port.

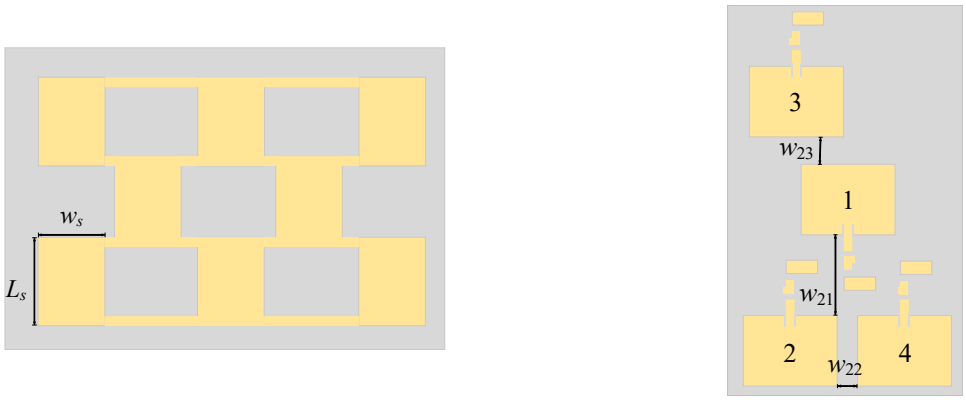

Figure 10. Diagram of the (**a**) microstrip grid rectenna and (**b**) compact rectenna array's local structure.

After determining the positions between each antenna, the output serpentine microstrip lines are adjusted to fit the optimized rectenna array structure. Additionally, considering the heating issue in the output branch lines, the output is designed to have four paths. This design increases the number of branches in the output DC circuit, reducing the DC energy per branch and thereby decreasing energy loss and potential experimental risks in the DC output circuit.

The final configuration is determined with radiating edge distance w_{21} = 37.5 mm, w_{23} = 15 mm, and transmission edge distance w_{22} = 15 mm. This distance between adjacent elements is significantly reduced compared to the half-wavelength (≈60 mm at 2.45 GHz) in traditional patch antenna arrays, achieving antenna array miniaturization. The simulated results for the scattering parameters $|S_{mn}|$ (where $m \neq n$ and $m, n = 1, 2, 3, 4$) are shown in Figure 11. It can be observed that the scattering parameters $|S_{mn}|$ are all less than −15 dB, indicating low coupling between the radiating patch units.

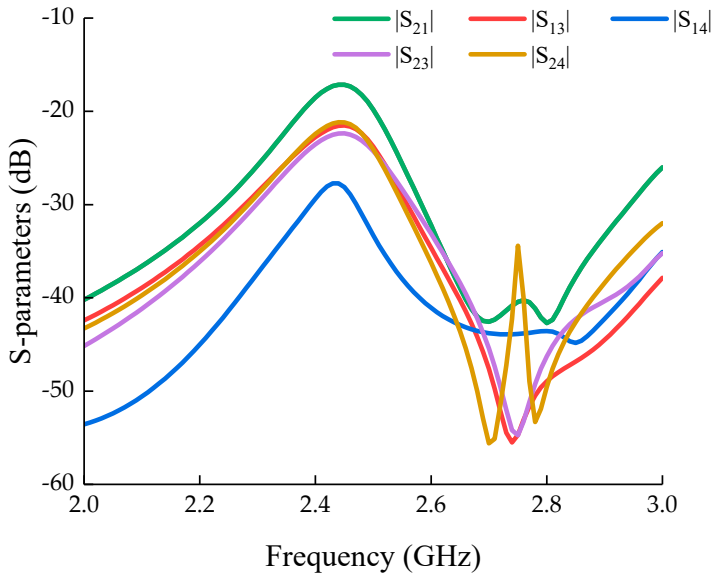

Figure 11. Simulation result of rectangular patch antenna's S-parameters.

3.2. Experiment and Analysis of the Proposed Compact Rectenna Array

To complete the design of the rectenna, the feeding ports of the rectangular patch antennas are connected to the microwave rectifier designed in the Section 2 and the corners of the serpentine microstrip line are adjusted. The final design and fabrication process of the 4 × 4 rectenna array are shown in Figure 12. In this design, the serpentine microstrip line functions both as the output filter for the rectifier and as the DC connection circuit between the rectenna units, allowing for a parallel connection between the DC outputs from the 16 rectenna units. The area of the rectenna array is 21.7 × 27.5 cm^2.

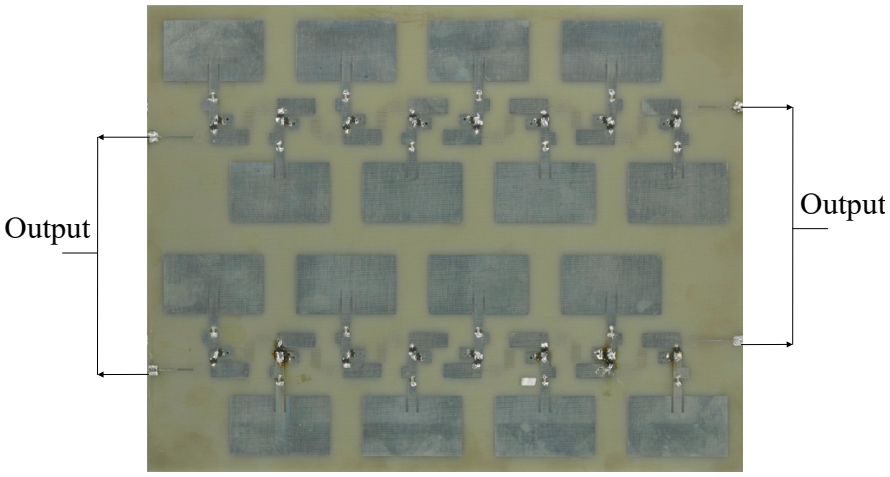

Figure 12. Photograph of the proposed rectenna array.

The experiment system for the rectenna array is shown in Figure 13. The testing uses an HMC-T2220 signal source (from Analog Devices Inc., Wilmington, NC, USA), a solid-state amplifier, a 16 dBi standard horn antenna, a multimeter, and a high-power load. The maximum output power of the microwave power source is 79.9 W. By adjusting the output power of the microwave source, the DC output power and rectification efficiency of the rectenna array are measured.

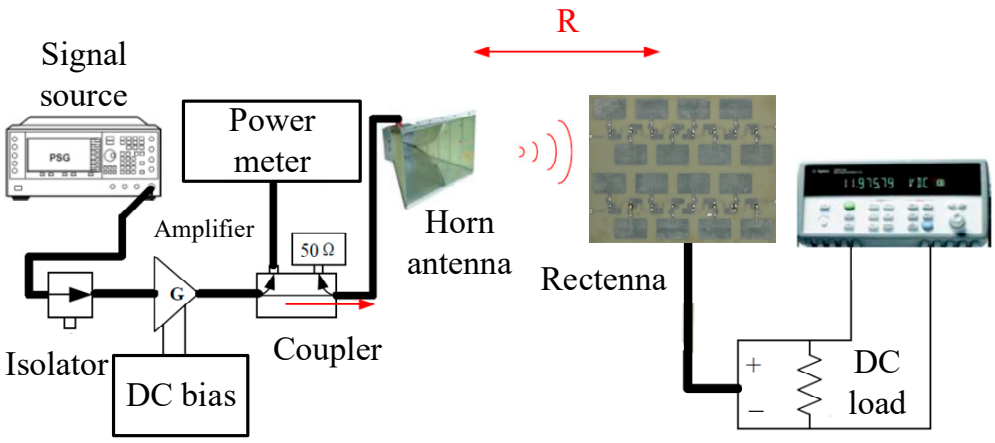

Figure 13. Diagram of experiment system.

The power density ρ_d of the microwave power that the rectenna array can receive at the test point is given as follows:

$$\rho_d = \frac{P_t G_t}{4\pi d^2} \tag{17}$$

where P_t is the microwave transmission power, G_t is the gain of the transmitting antenna, and d is the distance between the transmitting antenna and the receiving antenna. Therefore, the rectification efficiency η of the rectenna array can be calculated using the following equation:

$$\eta = \frac{P_{\text{out}}}{P_r} \times 100\% = \frac{{V_{out}}^2 / R_{Load}}{P_t G_t / 4\pi d^2 \times A_{rectenna-array}} \tag{18}$$

where P_{out} is the DC output power, P_r is the power that the rectenna array can receive, V_{out} is the DC output voltage, R_{Load} is the value of the DC load, and $A_{rectenna\text{-}array}$ is the area of the rectenna array.

The far-field region of the transmitting antenna is R = 0.5 m. The tested rectenna array is located within the far-field region of the transmitting antenna. The final test results of the rectenna array are shown in Figure 14. Figure 14a shows that the curve of the rectenna array's DC output power varies with the distance between the transmitting and receiving antennas when the microwave transmission power is 39.3 W, 66.6 W, and 79.9 W, respectively. From this figure, it can be seen that the optimized compact patch antenna array has a maximum DC output energy of 14.03 W. Figure 14b shows the rectenna array's rectification efficiency curve under different microwave transmission powers. The optimized compact patch antenna array achieves a maximum rectification efficiency of 47.6%. The maximum DC output of a single rectifier is 0.93 W. Therefore, according to the experiment results, the relative error between the measured power and the theoretical maximum output power of the rectenna array consisting of 16 rectifiers is 5.7%, which is closer to the theoretical value.

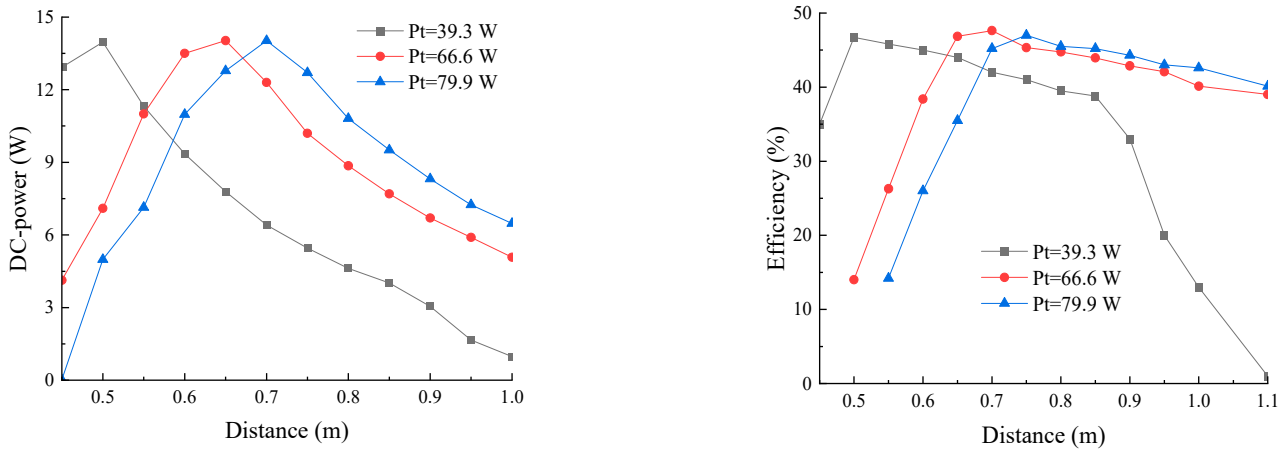

(**a**) (**b**)

Figure 14. Experimental results of the rectenna array. (**a**) Output DC power; (**b**) rectification efficiency.

Table 5 presents a comparison between our proposed rectenna and previous works. Although it does not stand out in terms of peak efficiency, our rectenna achieves a notably higher DC output power. Compared to other designs, even with the same number of elements, it maintains a significant advantage in terms of output power. This rectenna meets the requirements for wirelessly powering an LCD screen.

Table 5. Performance comparison of S-band rectennas.

	Center Frequency	Maximum Rectification Efficiency	Power Density at Best Efficiency	Maximum DC Output Power	Number of Elements
[34]	2.45 GHz	77.7%	0.5 mW/cm^2	0.097 W	2 × 2
[35]	2.45 GHz	60%	0.20 mW/cm^2	NM	Single
[36]	2.45 GHz	61%	0.29 mW/cm^2	NM	Single
This work	2.45 GHz	47.6%	49.28 mW/cm^2	14.03 W	4 × 4

NM: not mentioned.

4. Wireless Power Transmission Experiments and Results

Based on the two designed compact patch antenna arrays, in this section, we describe the implementation of a wireless power transmission and communication system. A diagram of the experimental system is shown in Figure 15. At the end of the transmission, microwaves are generated by a magnetron and emitted into free space by the transmitting antenna; this process is monitored by a microwave power meter. The communication signal generated by the signal source is also transmitted through the transmitting antenna. At the receiving end, the rectenna array collects and converts the microwave power into DC power to supply a 12-inch LCD screen, allowing the display to receive the communication signal and operate normally, producing an image.

The final wireless power transfer experiment test results are shown in Figure 16. As can be seen from the figure, in the wireless power transfer experiment, the compact rectenna array was able to power a 12-inch LCD screen with a rated power of 12 W at a transmission distance of 2 m. The LCD screen does not have any other power supply. This wireless power transmission experiment demonstrates the value of the compact rectenna array designed in this paper for MWPT systems.

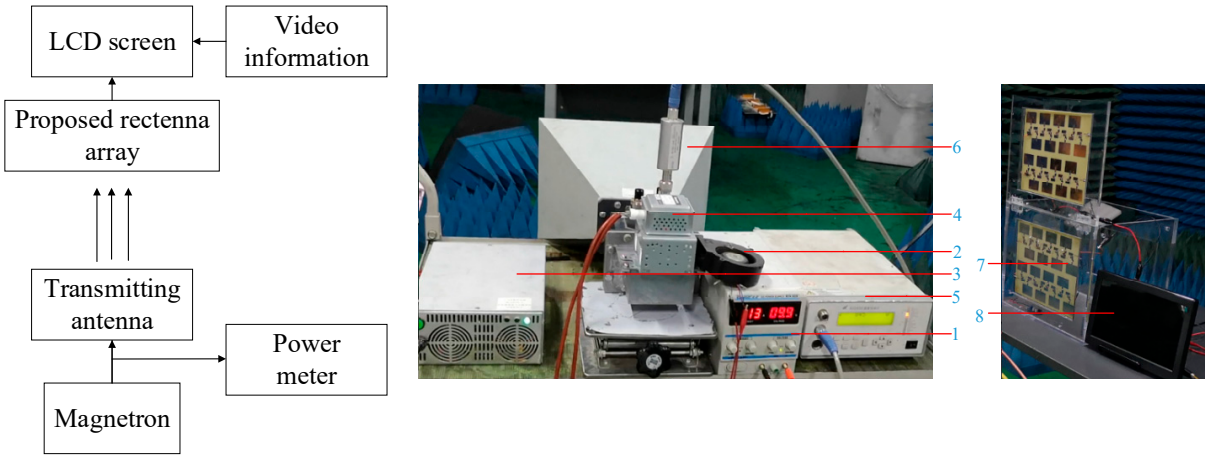

Figure 15. (**a**) Diagram and (**b**) photograph of wireless power transmission experimental system. (1. DC power supply, 2. magnetron cooling fan, 3. magnetron switch-mode power supply, 4. magnetron, 5. microwave power meter, 6. transmitting antenna, 7. proposed rectenna arrays, 8. 12-inch display screen).

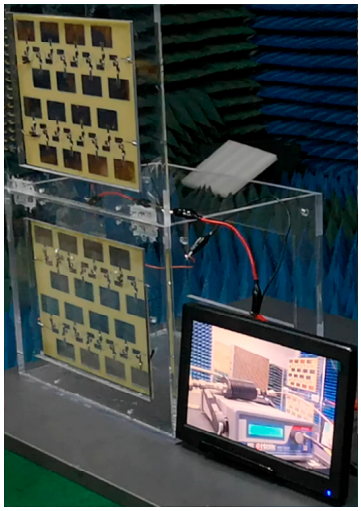

Figure 16. Wireless power transfer experiment result.

5. Conclusions

MWPT technology, as an emerging power transmission method, holds significant research value and promising development prospects. This technology can be applied to areas such as space solar power stations (SPSs), wireless charging ZigBee wireless sensors, and space microwave power recovery, making it highly valuable for development.

This paper studies and discusses the application of compact rectenna arrays in wireless power transmission systems and proposes a microwave rectifier using a serpentine microstrip line as the output filter. Compared to traditional microwave rectifiers that use patch capacitors as the output filter, this rectifier offers better consistency, easier array assembly, and a more compact structure. The research conducted in this paper led to the development of a compact rectenna array for wireless power transmission systems, which achieved an output of 117.6 mW/cm^3 in terms of DC power per unit volume.

Finally, this paper designed a wireless power transmission experimental system, successfully using the designed rectenna array as the receiving end to power a 12 W LCD screen. This experiment verified the feasibility of the proposed solution, demon-

strating its significant engineering value and application prospects in wireless power transmission systems.

Author Contributions: Conceptualization, D.H. and J.L.; methodology, Z.D. and D.H.; Simulation, J.L.; validation, J.L., D.H. and Z.H.; formal analysis, J.Z.; investigation, J.Z.; resources, D.H., C.L. and J.Z.; writing—original draft preparation, Z.H.; writing—review and editing, C.L.; visualization, Z.H.; supervision, J.Z.; project administration, C.L. and J.Z. All authors have read and agreed to the published version of the manuscript.

Funding: This work was supported in part by the National Natural Science Foundation of China under Grant 62071316.

Data Availability Statement: The original contributions presented in the study are included in the article, further inquiries can be directed to the corresponding author.

Conflicts of Interest: Author Dajiu Huang, Ziqiang Du and Ji Zhang were employed by the company China Telecom Group Co., Ltd. Sichuan Branch. The remaining authors declare that the research was conducted in the absence of any commercial or financial relationships that could be construed as a potential conflict of interest.

References

1. Martin, T.C.; Tesla, N. *The Inventions, Researches, and Writing of Nikola Tesla, with Special Reference to His Work in Polyphase Currents and High Potential Lighting*; Angriff Press: Los Angeles, CA, USA, 1894.
2. Fan, G.; Duan, B.; Zhang, Y.; Li, X.; Ji, X. Full-spectrum selective thin film-based photonic cooler for solar cells of space solar power station. *Acta Astronaut.* **2021**, *180*, 196–204. [CrossRef]
3. Takano, T. Antennas for a Space Solar Power System and Technical Challenges. In Proceedings of the 16th European Conference on Antennas and Propagation (EuCAP), Madrid, Spain, 11 May 2022. [CrossRef]
4. Wang, Y.; Wei, G.; Dong, Y.; Dong, S.; Yu, X.; Li, X. Analysis of Receiving Array and Rectifier for Megawatt SSPS. In Proceedings of the 2020 IEEE Wireless Power Transfer Conference (WPTC), Seoul, Republic of Korea, 24 December 2020. [CrossRef]
5. Huo, Y.; Dong, X.; Lu, T.; Xu, W.; Yuen, M. Distributed and Multilayer UAV Networks for Next-Generation Wireless Communication and Power Transfer: A Feasibility Study. *IEEE Internet Things J.* **2019**, *6*, 7103–7115. [CrossRef]
6. Miwatashi, K.; Shinohara, N.; Mitani, T. Design of Rectifier Circuit for Wireless Power Transfer to Pipeline Inspection Robots. In Proceedings of the 2020 IEEE Wireless Power Transfer Conference (WPTC), Seoul, Republic of Korea, 24 December 2020. [CrossRef]
7. Zhou, Y.; Zhou, H.; Zhou, F.; Wu, Y.; Leung, V.C.M. Resource Allocation for a Wireless Powered Integrated Radar and Communication System. *IEEE Wirel. Commun. Lett.* **2019**, *8*, 253–256. [CrossRef]
8. Liu, C.; Tan, F.; Zhang, H.; He, Q. A Novel Single-Diode Microwave Rectifier With a Series Band-Stop Structure. *IEEE Trans. Microw. Theory Tech.* **2017**, *65*, 600–606. [CrossRef]
9. Roberg, M.; Falkenstein, E.; Popović, Z. High-efficiency harmonically-terminated rectifier for wireless powering applications. In Proceedings of the 2012 IEEE/MTT-S International Microwave Symposium Digest, Montreal, QC, Canada, 17–22 June 2012; pp. 1–3. [CrossRef]
10. Liu, J.; Zhang, X.Y.; Yang, C.-L. Analysis and Design of Dual-Band Rectifier Using Novel Matching Network. *IEEE Trans. Circuits Syst. II Express Briefs* **2018**, *65*, 431–435. [CrossRef]
11. Lu, J.-J.; Yang, X.-X.; Mei, H.; Tan, C. A Four-Band Rectifier With Adaptive Power for Electromagnetic Energy Harvesting. *IEEE Microw. Wirel. Compon. Lett.* **2016**, *26*, 819–821. [CrossRef]
12. Kimionis, J.; Collado, A.; Tentzeris, M.M.; Georgiadis, A. Octave and Decade Printed UWB Rectifiers Based on Nonuniform Transmission Lines for Energy Harvesting. *IEEE Trans. Microw. Theory Tech.* **2017**, *65*, 4326–4334. [CrossRef]
13. He, Z.; Lan, J.; Liu, C. Compact Rectifiers With Ultra-wide Input Power Range Based on Nonlinear Impedance Characteristics of Schottky Diodes. *IEEE Trans. Power Electron.* **2021**, *36*, 7407–7411. [CrossRef]
14. Marian, V.; Vollaire, C.; Verdier, J.; Allard, B. Potentials of an Adaptive Rectenna Circuit. *IEEE Antennas Wirel. Propag. Lett.* **2011**, *10*, 1393–1396. [CrossRef]
15. Hu, Y.-Y.; Sun, S.; Su, H.-J.; Yang, S.; Hu, J. Dual-Beam Rectenna Based on a Short Series-Coupled Patch Array. *IEEE Trans. Antennas Propag.* **2021**, *69*, 5617–5630. [CrossRef]
16. Liu, C.; Lin, H.; He, Z.; Chen, Z. Compact Patch Rectennas Without Impedance Matching Network for Wireless Power Transmission. *IEEE Trans. Microw. Theory Tech.* **2022**, *70*, 2882–2890. [CrossRef]
17. Sun, H.; Guo, Y.-X.; He, M.; Zhong, Z. A Dual-Band Rectenna Using Broadband Yagi Antenna Array for Ambient RF Power Harvesting. *IEEE Antennas Wirel. Propag. Lett.* **2013**, *12*, 918–921. [CrossRef]
18. He, Z.; Lin, H.; Liu, C. Codesign of a Schottky Diode's and Loop Antenna's Impedances for Dual-Band Wireless Power Transmission. *IEEE Antennas Wirel. Propag. Lett.* **2020**, *19*, 1813–1817. [CrossRef]

19. Nakashima, N.; Sumiyoshi, T. A prototype of a 900 MHz band integrated rectenna by using a planar monopole antenna with feeder. *Radio Sci.* **2024**, *59*, 1–12. [CrossRef]
20. Zhang, X.; Cao, C.; Song, C. A Compact Dual-Band Dual-Circular-Polarization Wideband Rectenna Using Reverse Wilkinson Power Divider for Wireless Information and Power Transfer. *IEEE Antennas Wirel. Propag. Lett.* **2024**, *23*, 2728–2732. [CrossRef]
21. Khodaei, M.; Boutayeb, H.; Talbi, L. A High Efficiency and Ultra-Wideband Rectenna For RF Energy Harvesting Application. In Proceedings of the 18th European Conference on Antennas and Propagation (EuCAP), Glasgow, UK, 17–22 March 2024; pp. 1–4. [CrossRef]
22. Fernandez-Munoz, M.; Missous, M.; Sadeghi, M.; Lopez-Espi, P.L.; Sanchez-Montero, R.; Martinez-Rojas, J.A.; Diez-Jimenez, E. Fully Integrated Miniaturized Wireless Power Transfer Rectenna for Medical Applications Tested inside Biological Tissues. *Electronics* **2024**, *13*, 3159. [CrossRef]
23. Tiberi, T.; Fazzini, E.; Costanzo, A.; Masotti, D. Exploitation of Harmonic Generation in Time-Controlled Frequency-Diverse Arrays for WPT. *IEEE Trans. Antennas Propag.* **2024**, *72*, 497–505. [CrossRef]
24. Dhull, P.; Schreurs, D.; Paolini, G.; Costanzo, A.; Abolhasan, M.; Shariati, N. Multitone PSK Modulation Design for Simultaneous Wireless Information and Power Transfer. *IEEE Trans. Microw. Theory Tech.* **2024**, *72*, 446–460. [CrossRef]
25. Bolos, F.; Blanco, J.; Collado, A.; Georgiadis, A. RF Energy Harvesting From multi-Tone and Digitally Modulated Signals. *IEEE Trans. Microw. Theory Tech.* **2016**, *64*, 1918–1927. [CrossRef]
26. Ciccia, S.; Scionti, A.; Franco, G.; Giordanengo, G.; Terzo, O.; Vecchi, G. A Multi-Tone Rectenna System for Wireless Power Transfer. *Energies* **2020**, *13*, 2374. [CrossRef]
27. Pozar, D.M. *Microwave Engineering*; John Wiley and Sons: Hoboken, NJ, USA, 2006.
28. He, Z.; Yan, L.; Liu, C. An Adaptive Power Division Strategy for Nonlinear Components in Rectification. *IEEE Trans. Power Electron.* **2024**, *39*, 15436–15440. [CrossRef]
29. Niu, S.; Lyu, R.; Lyu, J.; Chau, K.T.; Liu, W.; Jian, L. Optimal Resonant Condition for Maximum Output Power in Tightly-Coupled WPT Systems Considering Harmonics. *IEEE Trans. Power Electron.* **2024**, 1–5. [CrossRef]
30. Yoo, T.-W.; Chang, K. Theoretical and experimental development of 10 and 35 GHz rectennas. *IEEE Trans. Microw. Theory Tech.* **1992**, *40*, 1259–1266. [CrossRef]
31. Lee, D.; Oh, J. Broad Dual-Band Rectifier With Wide Input Power Ranges for Wireless Power Transfer and Energy Harvesting. *IEEE Microw. Wirel. Compon. Lett.* **2022**, *32*, 599–602. [CrossRef]
32. He, Z.; Lin, H.; Zhu, H.; Liu, C. A Compact High-Efficiency Rectifier With a Simple Harmonic Suppression Structure. *IEEE Microw. Wirel. Compon. Lett.* **2020**, *30*, 1177–1180. [CrossRef]
33. Du, Z.-X.; Zhang, X.Y. High-Efficiency Microwave Rectifier With Less Sensitivity to Input Power Variation. *IEEE Microw. Wirel. Compon. Lett.* **2017**, *27*, 1001–1003. [CrossRef]
34. Li, X.; Yang, L.; Huang, L. Novel Design of 2.45-GHz Rectenna Element and Array for Wireless Power Transmission. *IEEE Access* **2019**, *7*, 28356–28362. [CrossRef]
35. Zhang, B.H.; Zhang, J.W.; Wu, Z.P.; Liu, C.G.; Zhang, B. A 2.45 GHz dielectric resonator rectenna for wireless power transmission. In Proceedings of the 2017 Sixth Asia-Pacific Conference on Antennas and Propagation (APCAP), Xi'an, China, 16–19 October 2017; pp. 1–3. [CrossRef]
36. Sun, H.; Geyi, W. A New Rectenna With All-Polarization-Receiving Capability for Wireless Power Transmission. *IEEE Antennas Wirel. Propag. Lett.* **2016**, *15*, 814–817. [CrossRef]